



## Article

# A New PM Sampler with a Built-In Black Carbon Continuous Monitor

Lorenzo Caponi <sup>1</sup>, Gianluca Cazzuli <sup>2</sup>, Giulio Gargioni <sup>2</sup>, Dario Massabò <sup>1,3,\*</sup> , Paolo Brotto <sup>1</sup> and Paolo Prati <sup>1,3</sup> 

<sup>1</sup> PM\_TEN srl, via Dodecaneso 33, 16146 Genoa, Italy; lorenzo.caponi@pm10-ambiente.it (L.C.); paolo.brotto@pm10-ambiente.it (P.B.); prati@ge.infn.it (P.P.)

<sup>2</sup> DADO LAB srl, via Pellizza da Volpedo 101A, 20092 Cinisello Balsamo, Italy; g.cazzuli@dadolab.com (G.C.); g.gargioni@dadolab.com (G.G.)

<sup>3</sup> Department of Physics and INFN, University of Genoa, Via Dodecaneso 33, 16146 Genoa, Italy

\* Correspondence: massabo@ge.infn.it

**Abstract:** We introduce a new instrument for sampling the airborne particulate matter (PM) while monitoring the black carbon (BC) atmospheric concentration. The concentration of PM and BC are usually measured by separate instruments with possible systematic differences even in the collecting inlets. The new equipment is based on a low-volume sequential PM sampler, fully compliant with the EU-CEN and US-EPA regulatory standards, with a built-in optical BC monitor. The BC concentration is continuously measured during the sampling in the PM accumulated on the filter while the PM concentration can be obtained off-line by a standard gravimetric analysis. The optical set-up, upstream the collecting filter, is composed by a single wavelength light source ( $\lambda = 635$  nm) and a photodiode, placed in way to receive the light backscattered by the filter surface at a fixed angle. The mechanical arrangement does not introduce any perturbation to the PM sampling. Thanks to an original calibration curve, the sample absorbance is deduced from the output signal of the photodiode. Finally, the BC concentration is obtained through the Mass Absorption Coefficient (MAC). After the sampling and the PM gravimetric determination, the same filter can be sent to other compositional analyses. Thermo-optical quantification of the Elemental and Organic Carbon (EC and OC) in the filter sample can thus be exploited to tune the MAC value to the PM composition of a particular site. The main features of the new instrument and the set of validation tests against other PM samplers and BC monitors of widespread use (i.e., Multi Angle Absorption Photometer and aethalometer) are detailed and discussed.

**Keywords:** black carbon; optical methods; PM samplers; real time monitors



**Citation:** Caponi, L.; Cazzuli, G.; Gargioni, G.; Massabò, D.; Brotto, P.; Prati, P. A New PM Sampler with a Built-In Black Carbon Continuous Monitor. *Atmosphere* **2022**, *13*, 299. <https://doi.org/10.3390/atmos13020299>

Academic Editor: Pasquale Avino

Received: 27 January 2022

Accepted: 5 February 2022

Published: 10 February 2022

**Publisher's Note:** MDPI stays neutral with regard to jurisdictional claims in published maps and institutional affiliations.



**Copyright:** © 2022 by the authors. Licensee MDPI, Basel, Switzerland. This article is an open access article distributed under the terms and conditions of the Creative Commons Attribution (CC BY) license (<https://creativecommons.org/licenses/by/4.0/>).

## 1. Introduction

The World Health Organization (WHO) included atmospheric particulate air pollution in the list of the most severe public health issues, mainly impacting in urban areas [1]. Carbonaceous aerosols are a major component of atmospheric particulate matter with significant impacts on health as well as on the total environment [2]. While present regulations [3] are worldwide based on the monitoring of the atmospheric concentration of PM<sub>10</sub> and PM<sub>2.5</sub> (i.e., mass concentration of particulate matter, PM, with aerodynamic diameter  $\leq 10$  and  $2.5$   $\mu\text{m}$ , respectively), the monitoring of the carbonaceous species inside the PM is more and more requested, even in view of possible new metrics to adopt for human health protection [4]. Combustion-related carbonaceous aerosols are thought to be more harmful to health than PM not generated by combustion [1,4]. Literature reviews [5] concluded that transport-related air pollution, rich in carbonaceous species, contributes to an increased risk of death, particularly from cardiopulmonary causes, and that it increases the risk of respiratory symptoms and diseases that are not related to allergies. Soot particles contribute to PM impact on human health; some effects are shared with other components but some works [6–9] suggested that there may be other specific impacts. Several works

stated adverse effects of soot on health [10–14], which include cardiopulmonary morbidity and mortality [15]. Typical size range of soot particles is the fine fraction that means breathable particulate. Thus, these particles are suspected to be particularly hazardous to human health, because they are sufficiently small to penetrate the membranes of the respiratory tract and enter the blood circulation or be transported along olfactory nerves into the brain [16,17]. A comprehensive and firm picture of the possible specific health effect of carbonaceous aerosol is still missing and good quality data are definitely necessary.

The literature on the measuring methodologies and equipment for carbonaceous aerosol is extremely wide with several comprehensive review articles [2,18,19]. So far, instruments to sample the PM on filters according to the standard regulations and on-line monitoring of the concentration of carbonaceous species (Elemental Carbon, EC, Organic Carbon, OC and Black Carbon, BC) have been separately and independently developed. Extremely diffused equipment, as the several generations of aethalometers [20] and/or the thermo-optical devices [21] do not allow to collect the PM on filters following the standard procedure on air quality monitoring (e.g., the European CEN EN 12341:1998).

In the last years, the Multi Wavelength Absorbance Analyzer, MWAA, [22,23] has been developed with the aim of performing a firm, non-destructive, black and brown carbon (BrC) determination [2,18,19] on PM samples collected on filter media. Brown carbon corresponds to a class of organic light-absorbing carbonaceous compounds with an imaginary part of the refractive index that increases moving toward short-visible and UV wavelengths [19], this resulting in a brownish or yellowish appearance. The MWAA instrument operates off-line and makes possible the determination of the concentration of the carbonaceous species in the same filter samples used for gravimetric and other speciation analyses [23,24], including thermo-optical OC and EC quantification.

The quantitative definition of the light absorbing properties of atmospheric aerosols is usually expressed by the mass absorption coefficient, MAC, which was firstly introduced by [4]. MAC is the light absorption cross section normalized to the mass of a given species (e.g., BC and/or BrC) of aerosol particles and it is given in units of ( $\text{m}^2 \text{g}^{-1}$ ). Hence, with a light beam impinging on a PM sample, the absorbed fraction (i.e., the absorbance of the filter sample, ABS) can be obtained as  $100 \cdot \text{ABS} = \text{MAC} \cdot t_{\text{BC}}$ , where MAC is the absorption coefficient of BC at the given wavelength and  $t_{\text{BC}}$  is the BC thickness on the filter (in  $\mu\text{g cm}^{-2}$ ).

The coupling of optical and thermo-optical analyses offers several advantages as the possibility to retrieve the MAC value [2,18,19] of the PM in a particular site [23] and to improve the accuracy in the OC/EC separation [23]. Finally, not neglecting the partial mismatching between BC and EC, the OC concentration could be simply determined as  $\text{OC} = \text{TC} - \text{BC}$ , with TC = total carbon retrieved from the thermal analysis only and BC determined by optical absorption. This is the approach of the Magee Scientific Carbonaceous Aerosol Speciation System, CASS, where a combined use of a Total Carbon Analyzer and of an Aethalometer provides a quasi-real-time determination of TC and BC, and hence of OC. Even disregarding the limitations of the aethalometer approach (the extinction adopted as proxy of the absorption, the need of situ-dependent corrections; [25,26] and references therein), the CASS does not allow the optical/thermal analysis on a filter sample suitable for a standard gravimetric determination of PM concentration.

Aiming to overcome present limitations, we designed, developed, and patented a new instrument by coupling a standard low-volume PM sampler with an optical module. The optical module monitors the BC concentration in the PM during the sampling on a 47-mm filter. The new instrument is fully compliant with the CEN standard and hence allows a direct correlation between PM and BC concentration in the same sample. The rationale of the method, the present set-up and the validation tests are thoroughly discussed in the next sections.

## 2. Materials and Methods

The characteristic feature of the new instrument, called GIANO\_BC<sub>1</sub><sup>TM</sup> (DADO LAB s.r.l., Milan, Italy), is the insertion of an optical set-up in the filter holder of a CEN compliant

sampling system. The optical module is composed of a laser diode and a photodiode to continuously measure the light absorption in the PM deposited on the filter. To not perturb the air flow and thus guarantee the respect of the CEN standard, both the laser diode and the photodiode are mounted upstream the filter, without any modification of the sample holder geometry. This way, the light absorption through the filter is retrieved from the monitoring of the light backscattered at a fixed angle and a calibration curve originally obtained by the MWAA instrument. A simplified view of the set-up is given in Figure 1. A single laser diode (nominal power = 10 mW) delivers a  $\lambda = 635$  nm beam to the sample surface and the light reflected at  $\theta = 125^\circ$  (angular acceptance =  $1.4^\circ$ ) is collected by a high-speed Si PIN photodiode.

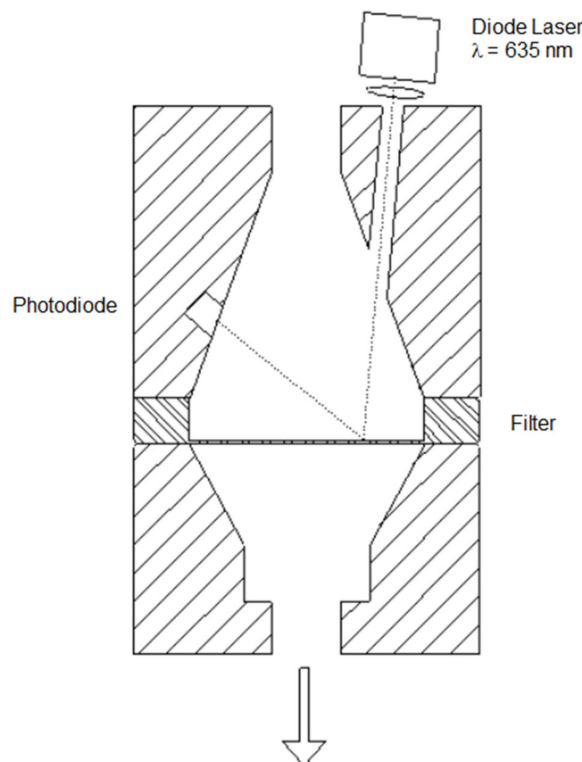


**Figure 1.** Layout of filter holder and optical module. The laser diode and the photodiode are positioned at  $5^\circ$  and  $125^\circ$ , respectively (relative to the perpendicular to the filter surface). The arrow marks the air flow direction.

The design of the new instrument benefits of the experience gained during the development of the MWAA, the latter retrieves the sample absorbance at any available wavelength from the signals of three photodiodes positioned at fixed angles [22,23]. It's the same scheme originally developed for the one-wavelength Multi Angle Absorption Photometer, MAAP [27]. So far, the analysis of the MWAA raw data led to a quantitative relationship between sample absorbance and light attenuation through the same filter sample [24,28]. To develop the new instrument, we assessed and exploited a relationship between sample absorbance (ABS) and reflectance (RFN). In our instrument, the photodiode is positioned at the same angle ( $\theta = 125^\circ$ , see Figure 1) of one of the two MWAA backward photodiodes. In this configuration, the non-linear relationship between ABS and RFN was retrieved by MWAA on a set of 240 PM samples collected on quartz and glass fiber filters and it is here reported in Figure 2. Samples exploited to deduce the calibration curve in Figure 2 came from several  $PM_{2.5}/PM_{10}$  sampling campaigns performed in sites of different type (i.e., rural, urban and urban background sites, [23,24,29]). The relationship between ABS and

RFN turned out to be very well described (i.e.,  $R^2 = 0.984$ ) by the quadratic curve given in Equation (1):

$$\text{ABS} = (0.209 \pm 0.006) \cdot \text{RFN}^2 + (0.249 \pm 0.005) \cdot \text{RFN} \quad (1)$$

with:

$$\text{RFN} = \ln \frac{I_0}{I} \quad (2)$$

and  $I_0$  and  $I$  being the intensity of the light beam diffused to the photodiode at  $\lambda = 125^\circ$  from the surface of the blank and exposed filter, respectively. As in any other filter-based optical method, the specific PM contribute ( $I$ ) has to be separated from that of the sampling filter through the ratio with the signal ( $I_0$ ) measured in the initial “blank” condition.

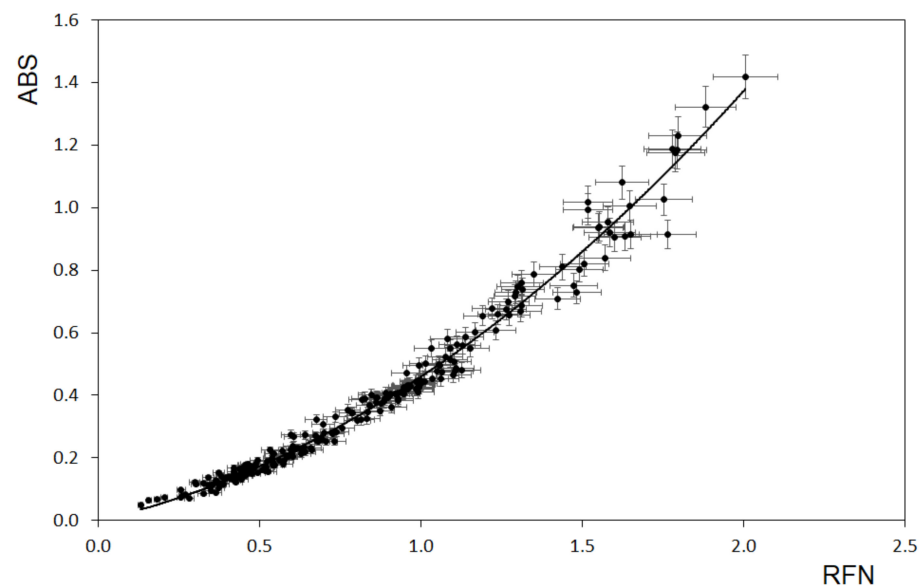


**Figure 2.** Absorbance (ABS) vs. reflectance (RFN) measured by the MWAA on a set on  $\text{PM}_{10}$  and  $\text{PM}_{2.5}$  samples collected on quartz fiber filters in different sites. Both the quantities are dimensionless. The equation of the fitting curve is given in the text.

The numeric values in Equation (2) are implemented in the instrument firmware. During the operation, the intensity of the diffused light beam is continuously measured resulting in a quasi-real-time monitoring. Each value of the light intensity used in Equation (2) is defined as the one-minute mean of the photodiode output voltage. During the sampling, after an initial wait to allow flow and filter surface stabilization (first minute), the values are recorded with a periodicity of 15 min. The recording interval can be varied by the user to optimize the sensitivity in different sites (e.g., highly polluted vs. rural or remote areas).

From each ABS value obtained by Equation (2), the absorption coefficient,  $b_{\text{abs}}$  [2,18,19] of the PM deposited on the filter is then calculated as:

$$b_{\text{abs}} = \text{ABS} \frac{S}{V} \quad (3)$$

where  $S$  = deposition surface,  $V$  = volume of sampled air. Finally, the BC atmospheric concentration is obtained through the:

$$\text{BC} \left[ \mu\text{g m}^{-3} \right] = \frac{b_{\text{abs}}}{\text{MAC}} \quad (4)$$

The MAC value is preset to  $6.6 \text{ m}^2 \text{ g}^{-1}$ , which is the same figure adopted in the MAAP instrument [27] but the parameter can be differently set by the user. This gives

the possibility of tuning to the peculiar composition of the PM in a given site, for instance through an off-line EC quantification on the same filters sampled during the BC monitoring.

The minimum detectable change of the photodiode output voltage turned out to be 0.6 mV, with a dynamic range of two decades (i.e., maximum output voltage = 60 mV). With a 24-h sampling at the CEN air flow of  $2.3 \text{ m}^3 \text{ h}^{-1}$ , the average BC atmospheric concentration leading to the saturation of the dynamic range is about  $17.7 \mu\text{g m}^{-3}$  (assuming  $\text{MAC} = 6.6 \text{ m}^2 \text{ g}^{-1}$ ). The Minimum Detection Limit (MDL) is defined as the variation of the BC thickness in the filter bringing to a 0.6 mV change in the photodiode output signal during the interval between two consecutive readings (15 min with the factory setting). Along the sampling period, it increases from the initial figure  $\text{MDL} = 0.4 \text{ ng cm}^{-2}$  to  $\text{MDL} = 10 \text{ ng cm}^{-2}$  at the 85% of the dynamic range and reaches about  $\text{MDL} = 200 \text{ ng cm}^{-2}$  near the saturation (all values calculated assuming  $\text{MAC} = 6.6 \text{ m}^2 \text{ g}^{-1}$ ).

As in any other similar set-up, the stability of the optical module (laser diode and photodiode) is potentially affected by temperature variations. Several tests were performed in operation conditions. With a temperature change of  $\pm 10 \text{ }^\circ\text{C}$ , the oscillation of the laser + photodiode response while monitoring a blank filter turned out to be  $< 3\%$ . This was included in the uncertainty budget of the BC concentration value.

The size of the laser beam spot on the filter surface is about 5 mm and the impact of possible not-homogeneous deposition must be considered. A set of 76 quartz fiber samples produced by the new instrument were analyzed by the MWAA  $125^\circ$ -photodiode too. Thanks to the micrometric MWAA set-up [22], the surface homogeneity could be studied over the whole filters surface and turned out to be  $(8 \pm 4)\%$ . Such figure was included in the overall uncertainty budget.

### 3. Results

While the measurements performed to obtain the calibration curves in Figure 2 refer to the development phase and are described in Section 2, we report in this section the results of the set of validation tests/campaigns performed on and with the new instrument.

The instrument design (i.e., the optical module insertion) did not modify the fluid dynamics features of a standard low volume PM sampler and therefore no effect/impact was expected on the sampling performance. However, we performed a test by deploying side-by-side a GIANO\_BC1<sup>TM</sup> ("new") and a GIANO<sup>TM</sup> ("ref", i.e., a standard low-volume sampler without the optical module) unit nearby an industrial site in Milan (Italy). The sampling campaign was carried out with quartz fiber filters (Whatman<sup>TM</sup>: WHA-1851-047 Grade QM-A, Cytiva, Marlborough, MA, USA) which were pre-conditioned for 2 days in a controlled room [temperature:  $(20 \pm 1) \text{ }^\circ\text{C}$ , relative humidity:  $(50 \pm 5)\%$ ] before and after the sampling and then weighed using an analytical balance (sensitivity:  $1 \mu\text{g}$ , electrostatic effects were avoided using a de-ionizing gun).  $\text{PM}_{2.5}$  and  $\text{PM}_{10}$  inlets were alternatively and together mounted on the two samplers. The results are reported in Figure 3 and show that the agreement between the gravimetric determination of the PM concentration is at the 2.5% level; correlation curve:  $new = (1.026 \pm 0.023) ref$ ;  $R^2 = 0.99$ . The agreement is well within the equivalence criteria fixed by the CEN standard (i.e., discrepancy on PM level  $< 10\%$ ) and is compatible with the intrinsic variability of the sampling efficiency of nominally identical PM samplers.

The second validation step was performed using two sets of daily  $\text{PM}_{10}$  samples (for a total of 76 quartz fiber filters) collected in spring 2019 in urban and urban background sites in the Italian cities of Bari, Genoa, and Milan, respectively. The instrument was equipped with a CEN  $\text{PM}_{10}$  inlet operated at an air flow of  $2.3 \text{ m}^3 \text{ h}^{-1}$ . In this case, the BC concentration (daily average) was compared with the outcome of the off-line analysis of the same filter samples performed by the reference MWAA set-up (at  $\lambda = 635 \text{ nm}$  only). The same MAC values were adopted in the two analyses and therefore the experiment directly compared the  $b_{\text{abs}}$  values retrieved by the new instrument and the full MWAA analysis [23]. The results are reported in Figure 4: the slope of the correlation curve turned out compatible with the unitary value;  $BC_{new} = (1.009 \pm 0.012) BC_{MWAA}$ ;  $R^2 = 0.988$ .

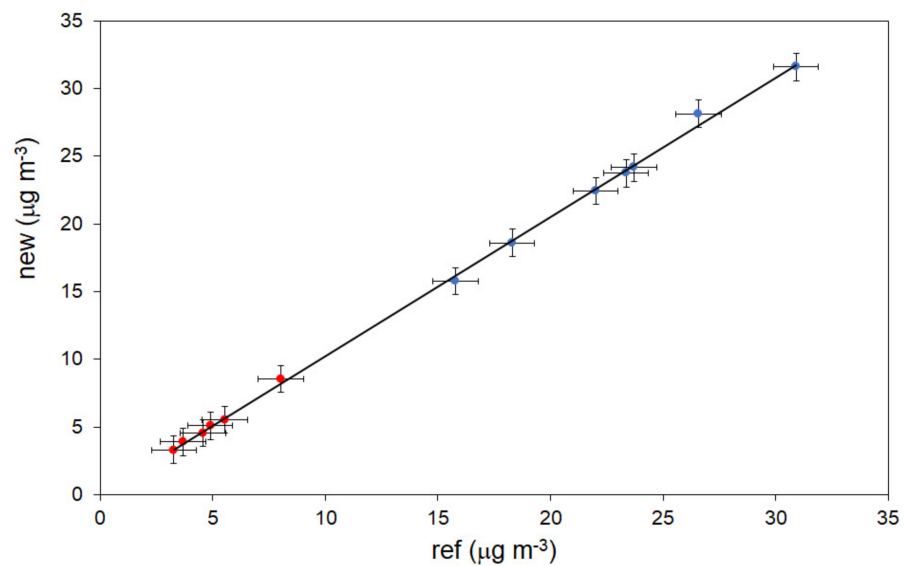


**Figure 3.** Intercomparison of the gravimetric  $PM_{2.5}$  (red points) and  $PM_{10}$  (blue points) concentration values measured on filter samples collected side-by-side by a standard (*ref*) and a new (*new*) sampler nearby an industrial site in Milan (Italy). The equation of the correlation curve is given in the text.

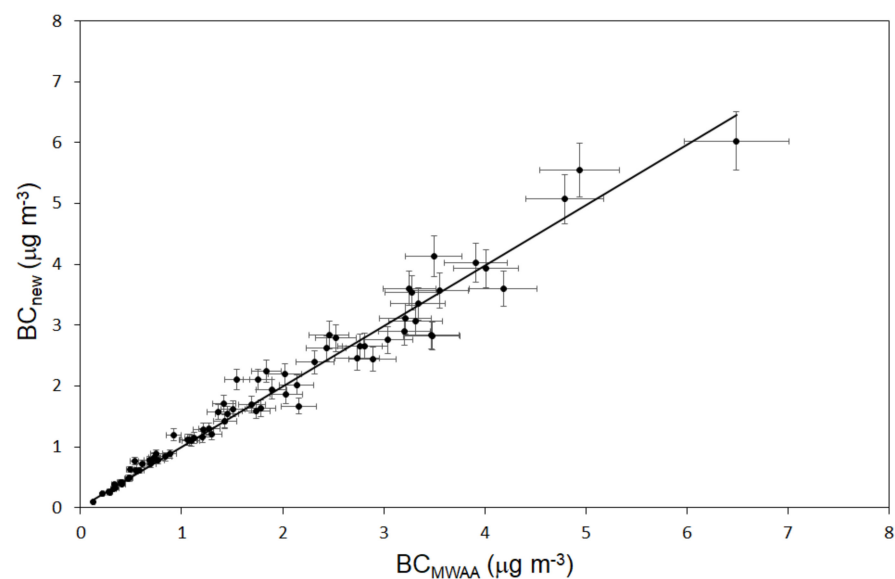


**Figure 4.** BC daily concentration measured on-line by the new instrument ( $BC_{new}$ ) and off-line by MWAA ( $BC_{MWAA}$ ) on a set of  $PM_{10}$  samples collected in urban and urban-background sites in the towns of Bari, Genoa, and Milan. The equation of the correlation curve is given in the text.

The third step of the validation path was a comparison with a MAAP unit. The new instrument and a MAAP were both equipped with US-EPA  $PM_{2.5}$  inlets (operated at an air flow of  $1 \text{ m}^3 \text{ h}^{-1}$ ) and deployed side-by-side in a background site, “Milano Celoria” (Lat  $45^\circ 28' 34.239'' \text{ N}$ ; Long  $9^\circ 13' 51.253'' \text{ E}$ ) in the urban area of Milan (Italy) for 22 days in February 2020. In Figure 5, we compare both the daily average and the hourly trend of the BC concentration measured by the two instruments set with the same MAC value. MAAP data were treated according to [30]. The time series of the BC daily average concentrations in the  $PM_{2.5}$  turned out to be extremely well correlated ( $R^2 = 0.99$ ) with  $BC_{new} = (1.10 \pm 0.04) BC_{MAAP}$ , as shown in Figure 5a. The analysis of the hourly time series revealed larger discrepancies ( $<20\%$  of the mean of the two values) in association with peak hours (Figure 5b). Furthermore, even if the new instrument deposited the PM on the



same filter for 24 h, the amplitude of the optical signal remained within the instrumental sensitivity for the whole period and despite the quite high BC concentration typical of the site.

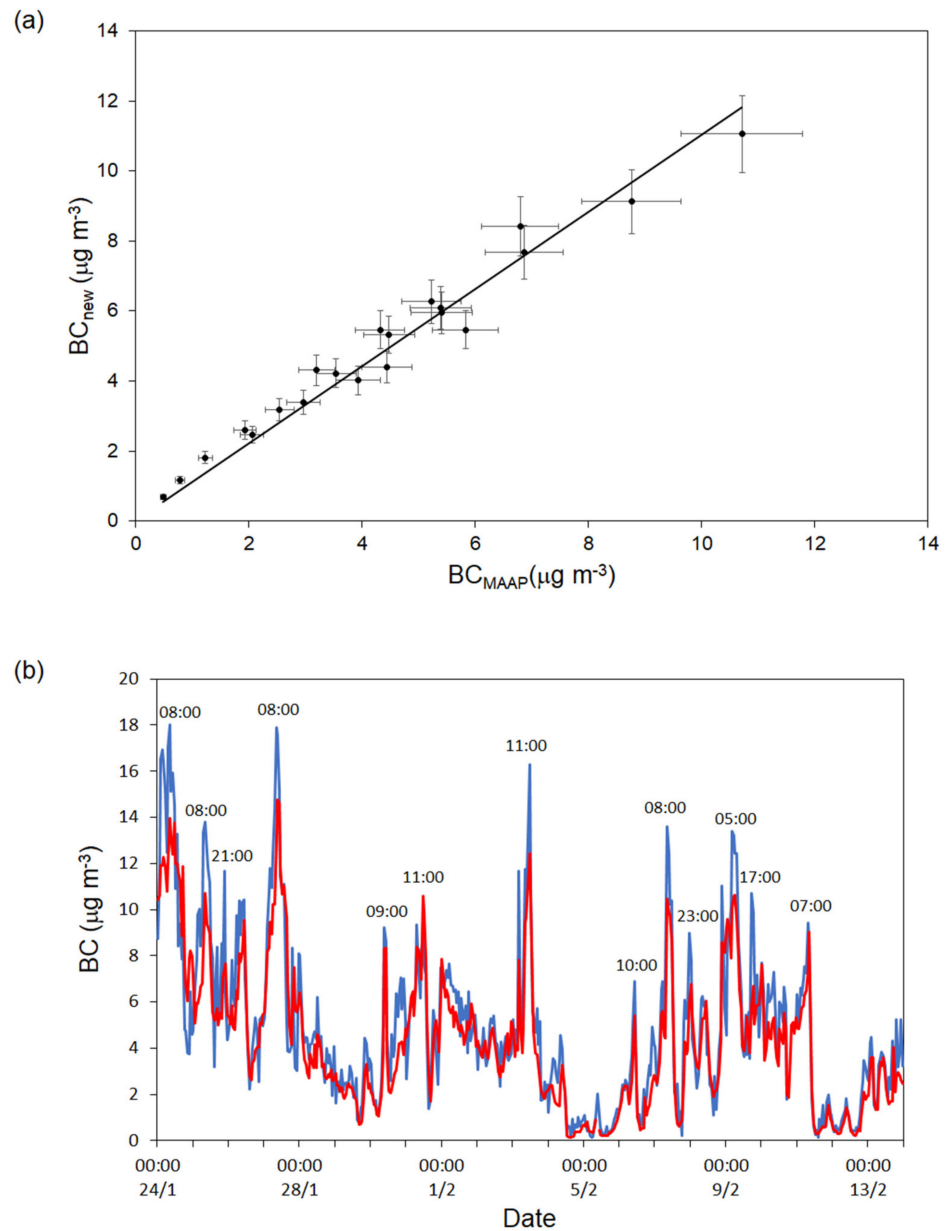


**Figure 5.** BC (in  $\text{PM}_{2.5}$ ) concentration time series measured by the new instrument ( $BC_{new}$ ) and a MAAP ( $BC_{MAAP}$ ) in an urban-background site in Milan (Italy), (a) daily average and (b) hourly trend (blue = *new*, red = *MAAP*, numeric labels identify peak hours). The equation of the correlation curve in panel (a) is given in the text.

At the conclusion of the field campaign, the filter samples were analyzed retrieving first the gravimetric  $\text{PM}_{2.5}$  concentration and then the EC/OC content by a thermo-optical analysis using a SUNSET EC/OC instrument [21] operated with the EUSAAR\_2 protocol [31]. In this way, the correlation between the daily mean of the  $b_{abs}$  values measured by new instrument and the EC concentration in  $\text{PM}_{2.5}$  could be studied (Figure 6a). The MAC value turned out almost double ( $\text{MAC} = 12.8 \pm 0.3 \text{ m}^2 \text{ g}^{-1}$ ) of the figure set in the MAAP but in the range of several other literature values ([18,22] and references therein) obtained at the same wavelength and, in some cases, in the same site ( $\text{MAC} = 10.4 \pm 0.3 \text{ m}^2 \text{ g}^{-1}$  [22]). With the site-specific MAC value set in our instrument, the BC concentration resulted

about one-half of those delivered by the MAAP (Figure 6b) and its contribute to  $PM_{2.5}$  was  $(4.2 \pm 1.3)\%$ .

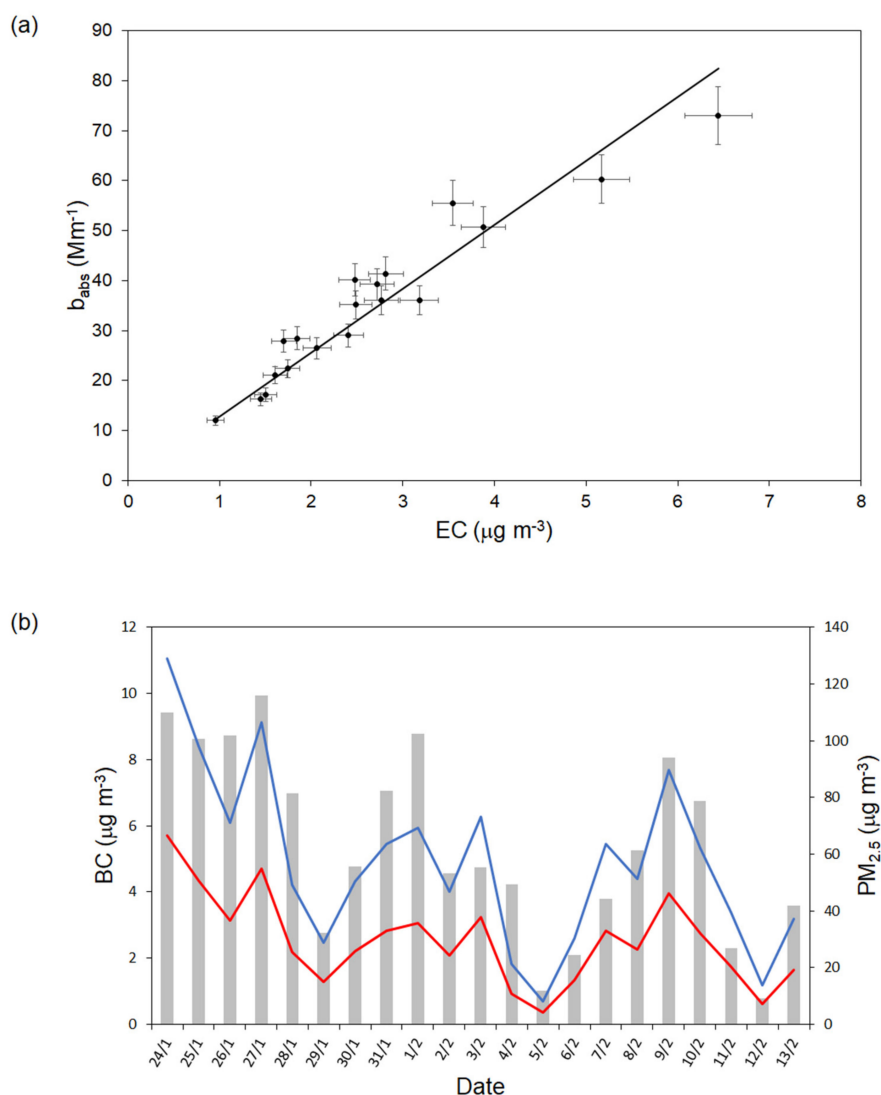


**Figure 6.** (a)  $b_{abs}$  values (daily average) measured by the new instrument vs. EC concentration measured by a thermo-optical analysis on a set of  $PM_{2.5}$  samples collected in an urban site in the city of Milan (Italy) in winter 2020; (b) BC concentration and  $PM_{2.5}$  daily trend (right axis) for the same set of samples. The blue and red lines show the BC concentration values (left axis) determined with a (standard) MAC of  $6.6 m^2 g^{-1}$  and  $12.8 m^2 g^{-1}$  (site specific), respectively. Grey bars indicate the  $PM_{2.5}$  level. The equation of the correlation curve in panel (a) is given in the text.

Finally, the new instrument was deployed side-by-side with a 7- $\lambda$  aethalometer (Magee Scientifics (Berkeley, CA, USA), model AE33) during a one-month (from 8 April to 6 May 2021) campaign managed by the Environmental Protection Agency of Lombardia Region, ARPAL (Italy). The sampling site (“Milano Marche”) is an urban traffic station located in the northeastern part of the external ring road (Lat  $45^{\circ}29'46.76''$  N, Long  $9^{\circ}11'27.43''$  E) of the city of Milan (IT), characterized for heavy traffic. In Figure 7, the correlation curve between hourly BC concentration values measured in  $PM_{10}$  by our instrument and by the aethalometer (at  $\lambda = 880$  nm) is shown. The two-time series resulted well correlated ( $R^2 = 0.95$ ), with an average 45% discrepancy, i.e.,  $BC_{aethal} = (1.45 \pm 0.01) BC_{new}$ . During the sampling, our instrument was operated with a CEN inlet (i.e., air flow =  $2.3 m^3 h^{-1}$ ) on a 12-h basis.



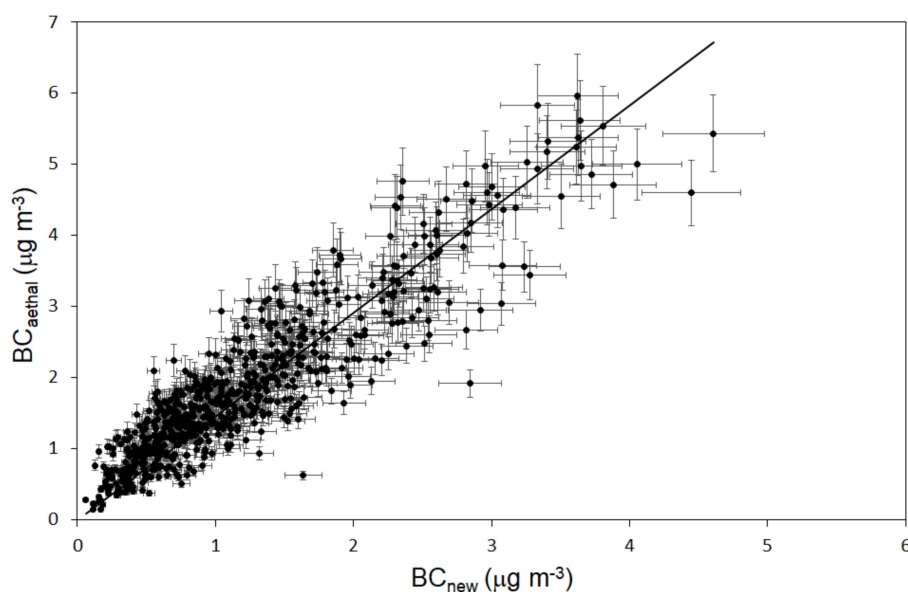


**Figure 7.** Hourly BC concentration values measured in a heavy traffic site in Milan by the new instrument ( $BC_{new}$ ) and an aethalometer ( $BC_{aethal}$ ) at  $\lambda = 880$  nm. The equation of the correlation curve is given in the text.

Off-line, the quartz fiber samples were analyzed by a thermo-optical analysis performed with a SUNSET Lab. Instrument and a NIOSH protocol [21]. The unit delivered the usual EC and OC concentration values and the so-called “Optical EC”,  $EC_{opt}$ . In this case, the SUNSET laser transmission is measured before and after the analysis cycle, and the difference is related to EC concentration via calibration. A predetermined calibration factor, based on numerous ambient measurements, is used to convert laser attenuation to EC mass on the filter [32]. Figure 8 reports the correlation curves between the two parameters provided by the thermo-optical analysis (EC, Figure 8a, and  $EC_{opt}$ , Figure 8b) and the 12-h averages of the two BC monitors (the new instrument and the aethalometer). In all the cases, the correlation coefficient turned out very high (i.e.,  $R^2 = 0.99$ ), with the aethalometer values again higher than the BC concentrations obtained through our new instrument:  $BC_{aethal} = (1.96 \pm 0.03) EC$ ;  $BC_{new} = (1.29 \pm 0.02) EC$ ;  $BC_{aethal} = (1.52 \pm 0.02) EC_{opt}$ ;  $BC_{new} = (1.01 \pm 0.01) EC_{opt}$ .

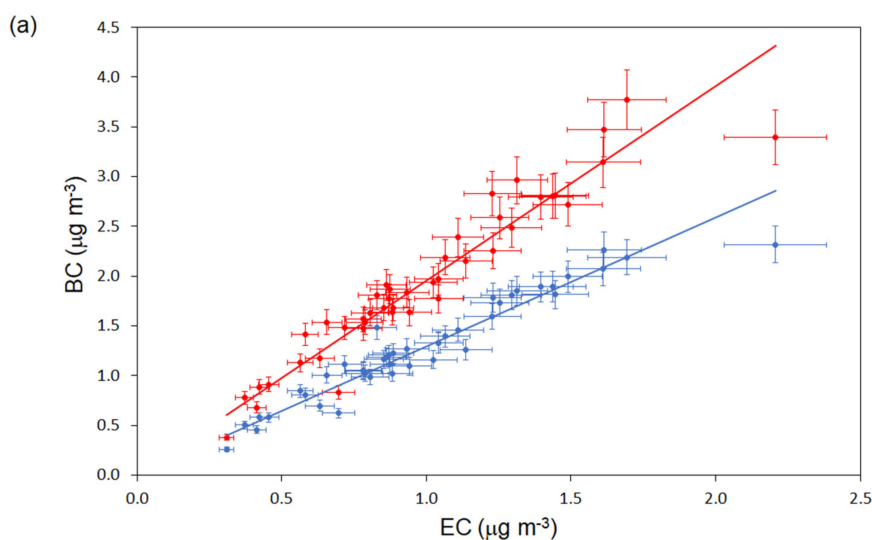


**Figure 8.** Cont.

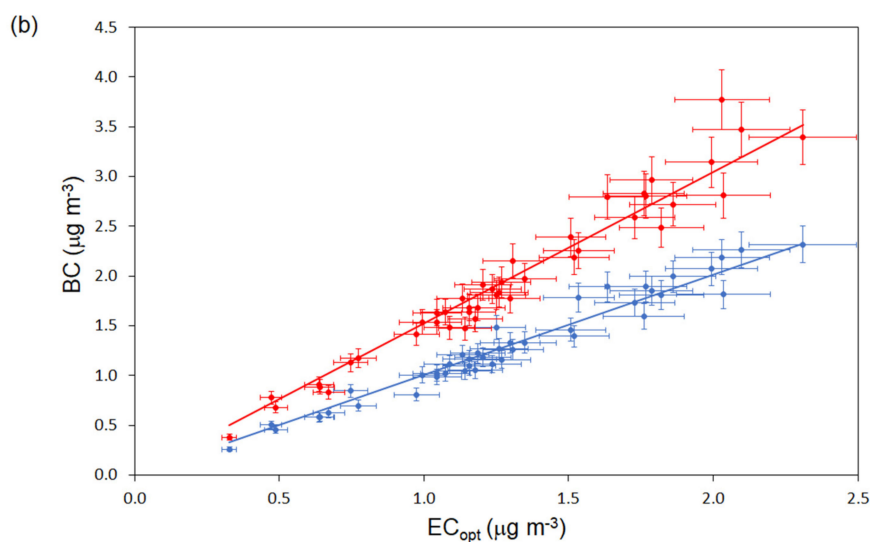


**Figure 8.** Correlation curve between the BC concentration values (12-h average) measured by our new instrument (blue points) and a 7- $\lambda$  aethalometer (red points) with the EC (a) and the  $EC_{opt}$  (b) concentration provided by the thermo-optical analysis of the  $PM_{10}$  samples. The equations of the correlation curves are given in the text.

#### 4. Discussion

The set of tests performed on the new instrument demonstrated that the optical setup upstream the filter holder does not perturb the PM collection and hence allows a reliable coupling of sampling and BC monitoring. Even with the detection of the light reflected at a sole angle, the internal calibration curve gives the possibility to retrieve the sample absorbance and hence the BC concentration value with the same accuracy (i.e., slope of the correlation curve compatible with a unitary value) of more complex instruments like the MWAAs.

Monitoring campaigns conducted deploying side-by-side the new instrument and MAAP and aethalometer units also revealed a good correlation between the time series of BC concentration values measured by the different monitors. The level of agreement turned out to be comparable to what reported for similar instrumentation in previous literature studies and reviews [2,21].

Off-line thermo-optical analyses were performed by standard SUNSET OC/EC analyzers on the quartz fiber filter samples collected in two different sites and seasons in the urban area of Milan. The correlation between our optical BC and the thermal EC concentration was again quite high even if the slope (i.e., the MAC value) showed a remarkable dependence on the sampling site. In an urban background site, wintertime, resulted  $MAC = 12.8 \text{ m}^2 \text{ g}^{-1}$  while the data reduction suggested  $MAC = 8.5 \text{ m}^2 \text{ g}^{-1}$  in a heavy traffic site, springtime. The latter is much closer to the GIANO\_BC1<sup>TM</sup> and MAAP factory setting ( $MAC = 6.6 \text{ m}^2 \text{ g}^{-1}$ ), originally fixed in the work by Petzold and Schönlinner by calibration with BC generated in a spark discharge (PALAS BC aerosol, [27]). The variability of ambient BC MAC does not surprise: it has been observed in several previous works (e.g., [18,22]) and could also partially depend on the different protocols adopted in the thermo-optical analyses ([28] and references therein). With our instrument, optical BC and EC can be measured on the same PM samples giving the possibility to tune the MAC to the characteristics of the specific site. It is noteworthy the extreme good agreement revealed in the heavy traffic site between BC and “optical EC” provided as by-product by the thermo-optical analysis.

Differently from other black carbon on-line monitors, for instance the aethalometer and the MAAP, our instrument deposits the PM on the same filter for the whole sampling period. In highly polluted sites (roughly: mean BC concentration  $\geq 6 \text{ } \mu\text{g m}^{-3}$ ), this feature could lead to a saturation of the optical absorbance signal before the conclusion of the

sampling. Such issue can be managed either reducing the sampling flow (i.e., adopting US-EPA inlets and air flow of  $1 \text{ m}^3 \text{ h}^{-1}$ ) or the sampling time.

## 5. Conclusions

GIANO\_BC<sub>1</sub><sup>TM</sup> is a new instrument for monitoring and research on atmospheric particulate matter. It couples a standard CEN sequential PM sampler with an optical module for quasi real-time monitoring of the black carbon concentration in the PM deposited on a 47 mm quartz fiber filter during the sampling. To our knowledge, this is the first and sole instrument on the market with such features. The GIANO\_BC<sub>1</sub><sup>TM</sup> key characteristics are the possibility to perform a PM<sub>2.5</sub> or PM<sub>10</sub> sampling fully compliant with the CEN standard while measuring, exactly on the same PM, the absorption coefficient and hence the BC concentration in the atmosphere. After the sampling, the filters remain available for gravimetric and other compositional analyses, in particular for EC/OC determination through the largely diffused thermo-optical methodology. This gives the possibility to measure the MAC value of the PM in a specific site and to calibrate the relationship between PM absorption coefficient and BC concentration, on the whole set of samples or on a suitable subset.

## 6. Patents

The GIANO\_BC<sub>1</sub><sup>TM</sup> innovative features and the technologies have been patented in Italy, patent number 10201900006685, date of deposit 09/05/2019; date of publication 09/11/2020, patent title:

Dispositivo e metodo per misurare la concentrazione di carbonio elementare nel particolato atmosferico.

**Author Contributions:** L.C., D.M. and P.P. conceived the idea of exploiting the optical reflectance, G.C. and G.G. designed the optical set-up; L.C., D.M. and P.B. performed all the validation experiments; L.C. and P.P. prepared the manuscript with contributions from all co-authors. All the co-authors shared and discussed the idea and the development of the new instrument. All authors have read and agreed to the published version of the manuscript.

**Funding:** This research received no external funding.

**Institutional Review Board Statement:** Not applicable.

**Informed Consent Statement:** Not applicable.

**Data Availability Statement:** Data supporting results are available at: <https://labfisa.ge.infn.it/index.php/data-repository?view=document&id=8:research-data-for-manuscript-id-atmosphere-1594016&catid=10> (accessed on 11 January 2022).

**Acknowledgments:** The Authors are indebted with the researchers of the Environmental Physics group of the University of Milan (<http://eng.fisica.unimi.it/ecm/home/research/research-groups/applied-physics/physics-of-climate-and-environment> (accessed on 11 January 2022)) for the use of the MAAP and the assistance in its data reduction and with ARPAL, in particular of Cristina Colombi, for the management of the campaign in the Milano-Marche site and the thermo-optical analyses to measure the elemental carbon concentration.

**Conflicts of Interest:** As the affiliations underlined, the potential competing interests could depend on: Gianluca Cazzuli and Giulio Gargioni are partners and employees of the company DadoLab s.r.l. which is the company that markets the instrument presented in this work; Paolo Brotto and Lorenzo Caponi are respectively partner and employee of PM\_TEN s.r.l. which is a company commercially connected to DadoLab s.r.l.; Paolo Prati and Dario Massabò are currently partners of the company PM\_TEN s.r.l.

## References

1. World Health Organization: Ambient Air Pollution. A Global Assessment of Exposure and Burden of Disease. 2016. Available online: <https://www.who.int/phe/publications/air-pollution-global-assessment/en/> (accessed on 26 March 2021).
2. Massabò, D.; Prati, P. An overview of optical and thermal methods for the characterization of carbonaceous aerosol. *La Rivista del Nuovo Cimento* **2021**, *44*, 145–192. [[CrossRef](#)]
3. EC Directive 2008/50. Directive on Ambient Air Quality and Cleaner Air for Europe. 2018. Available online: <https://eur-lex.europa.eu>. (accessed on 23 November 2021).
4. Janssen, N.A.H.; Gerard, H.; Simic-Lawson, M.; Fischer, P.; van Bree, L.; ten Brink, H.; Keuken, M.; Atkinson, R.W.; Ross Anderson, H.R.; Brunekreef, B.; et al. Black Carbon as an Additional Indicator of the Adverse Health Effects of Airborne Particles Compared with PM10 and PM2.5. *Environ. Health Perspect.* **2011**, *119*, 1691–1699. [[CrossRef](#)] [[PubMed](#)]
5. Krzyzanowski, M.; Kuna-Dibbert, B.; Schneider, J. *Health Effects of Transport-Related Air Pollution*; World Health Organization: Copenhagen, Denmark, 2005.
6. Costabile, F.; Alas, H.; Aufderheide, M.; Avino, P.; Amato, F.; Argentini, S.; Barnaba, F.; Berico, M.; Bernardoni, V.; Biondi, R.; et al. First Results of the “Carbonaceous Aerosol in Rome and Environs (CARE)” Experiment: Beyond Current Standards for PM10. *Atmosphere* **2017**, *8*, 249. [[CrossRef](#)]
7. Fuzzi, S.; Baltensperger, U.; Carslaw, K.; Decesari, S.; Denier van der Gon, H.; Facchini, M.C.; Fowler, D.; Koren, I.; Langford, B.; Lohmann, U.; et al. Particulate matter, air quality and climate: Lessons learned and future needs. *Atmos. Chem. Phys.* **2015**, *15*, 8217–8299. [[CrossRef](#)]
8. Olstrup, H.; Forsberg, B.; Orru, H.; Spanne, M.; Nguyen, H.; Molnár, P.; and Johansson, C. Trends in air pollutants and health impacts in three Swedish cities over the past three decades. *Atmos. Chem. Phys.* **2018**, *18*, 15705–15723. [[CrossRef](#)]
9. Segerström, D.; Eneroth, K.; Gidhagen, L.; Johansson, C.; Omstedt, G.; Nylén, A.E.; Forsberg, B. Health Impact of PM10, PM2.5 and Black Carbon Exposure Due to Different Source Sectors in Stockholm, Gothenburg and Umea, Sweden. *Int. J. Environ. Res. Public Health* **2017**, *14*, 742. [[CrossRef](#)]
10. Anenberg, S.C.; Horowitz, L.W.; Tong, D.Q.; West, J.J. An estimate of the global burden of anthropogenic ozone and fine particulate matter on premature human mortality using atmospheric modeling. *Environ. Health Perspect.* **2010**, *118*, 1189–1195. [[CrossRef](#)]
11. Cassee, F.R.; Héroux, M.E.; Gerlofs-Nijland, M.E.; Kelly, F.J. Particulate matter beyond mass: Recent health evidence on the role of fractions, chemical constituents and sources of emission. *Inhal. Toxicol.* **2013**, *25*, 802–812. [[CrossRef](#)]
12. Gan, C.M.; Wu, Y.; Madhavan, B.L.; Gross, B.; Moshary, F. Application of active optical sensors to probe the vertical structure of the urban boundary layer and assess anomalies in air quality model PM2.5 forecasts. *Atmos. Environ.* **2011**, *45*, 6613–6621. [[CrossRef](#)]
13. Lelieveld, J.; Evans, J.; Fnais, M. The contribution of outdoor air pollution sources to premature mortality on a global scale. *Nature* **2015**, *525*, 367–371. [[CrossRef](#)]
14. Pope, C.A., III; Burnett, R.T.; Thun, M.J. Lung Cancer, Cardiopulmonary Mortality, and Long-term Exposure to Fine Particulate Air Pollution. *JAMA* **2002**, *287*, 1132–1141. [[CrossRef](#)] [[PubMed](#)]
15. Janssen, N.A.H.; Fischer, P.; Marra, M.; Ameling, C.; Cassee, F.R. Short-term effects of PM2.5, PM10 and PM2.5–10 on daily mortality in the Netherlands. *Sci. Total Environ.* **2013**, *463*, 20–26. [[CrossRef](#)] [[PubMed](#)]
16. Nemmar, A.; Hoet, P.H.M.; Vanquickenborne, B.; Dinsdale, D.; Thomeer, M.; Hoylaerts, M.F.; Vanbilloen, H.; Mortelmans, L.; Nemery, B. Passage of Inhaled Particles Into the Blood Circulation in Humans. *Circulation* **2002**, *105*, 411–414. [[CrossRef](#)] [[PubMed](#)]
17. Oberdörster, G.; Maynard, A.; Donaldson, K. Principles for characterizing the potential human health effects from exposure to nanomaterials: Elements of a screening strategy. *Part. Fibre Toxicol.* **2005**, *2*, 8. [[CrossRef](#)]
18. Bond, T.; Bergstrom, R.W. Light absorption by carbonaceous particles: An investigative review. *Aerosol Sci. Technol.* **2006**, *40*, 27–67. [[CrossRef](#)]
19. Moosmüller, H.; Chakrabarty, R.K.; Arnott, W.P. Aerosol light absorption and its measurement: A review. *J. Quant. Spectrosc. Ra.* **2009**, *110*, 844–878. [[CrossRef](#)]
20. Hansen, A.D.A.; Rosen, H.; Novakov, T. Aethalometer: An instrument for the real-time measurement of optical absorption by aerosol particles. *Sci. Total Environ.* **1984**, *36*, 191–196. [[CrossRef](#)]
21. Birch, M.E.; Cary, R.A. Elemental carbon-based method for monitoring occupational exposures to particulate diesel exhaust. *Aerosol Sci. Technol.* **1996**, *25*, 221–241. [[CrossRef](#)]
22. Massabò, D.; Bernardoni, V.; Bove, M.C.; Brunengo, A.; Cuccia, E.; Piazzalunga, A.; Prati, P.; Valli, G.; Vecchi, R. A multi-wavelength optical set-up for the characterization of carbonaceous particulate matter. *J. Aerosol Sci.* **2013**, *60*, 34–46. [[CrossRef](#)]
23. Massabò, D.; Caponi, L.; Bernardoni, V.; Bove, M.C.; Brotto, P.; Calzolari, G.; Cassola, F.; Chiari, M.; Fedi, M.E.; Fermo, P.; et al. Multi-wavelength optical determination of black and brown carbon in atmospheric aerosols. *Atmos. Environ.* **2015**, *108*, 1–12. [[CrossRef](#)]
24. Massabò, D.; Caponi, L.; Bove, M.C.; Prati, P. Brown carbon and thermal-optical analysis: A correction based on optical multi-wavelength apportionment of atmospheric aerosols. *Atmos. Environ.* **2016**, *125*, 119–125. [[CrossRef](#)]
25. Collaud Coen, M.; Weingartner, E.; Apituley, A.; Ceburnis, D.; Fierz-Schmidhauser, R.; Flentje, H.; Henzing, J.S.; Jennings, S.G.; Moerman, M.; Petzold, A.; et al. Minimizing light absorption measurement artifacts of the Aethalometer: Evaluation of five correction algorithms. *Atmos. Meas. Tech.* **2010**, *3*, 457–474. [[CrossRef](#)]

26. Saturno, J.; Pöhlker, C.; Massabò, D.; Brito, J.; Carbone, S.; Cheng, Y.; Chi, X.; Ditas, F.; Hrabě de Angelis, I.; Morán-Zuloaga, D.; et al. Comparison of different Aethalometer correction schemes and a reference multi-wavelength absorption technique for ambient aerosol data. *Atmos. Meas. Tech.* **2017**, *10*, 2837–2850. [[CrossRef](#)]
27. Petzold, A.; Schölinner, M. Multi-angle absorption photometry—A new method for the measurement of aerosol light absorption and atmospheric black carbon. *J. Aerosol Sci.* **2004**, *35*, 421–441. [[CrossRef](#)]
28. Massabò, D.; Altomari, A.; Vernocchi, V.; Prati, P. Two-wavelength thermal–optical determination of light-absorbing carbon in atmospheric aerosols. *Atmos. Meas. Tech.* **2019**, *12*, 3173–3182. [[CrossRef](#)]
29. Bernardoni, V.; Pileci, R.E.; Caponi, L.; Massabò, D. The Multi-Wavelength Absorption Analyzer (MWA) Model as a Tool for Source and Component Apportionment Based on Aerosol Absorption Properties: Application to Samples Collected in Different Environments. *Atmosphere* **2017**, *8*, 218. [[CrossRef](#)]
30. Hyvärinen, A.-P.; Vakkari, V.; Laakso, L.; Hooda, R.K.; Sharma, V.P.; Panwar, T.S.; Beukes, J.P.; van Zyl, P.G.; Josipovic, M.; Garland, R.M.; et al. Correction for a measurement artifact of the Multi-Angle Absorption Photometer (MAAP) at high black carbon mass concentration levels. *Atmos. Meas. Tech.* **2013**, *6*, 81–90. [[CrossRef](#)]
31. Cavalli, F.; Viana, M.; Yttri, K.E.; Genberg, J.; Putaud, J.-P. Toward a standardised thermal-optical protocol for measuring atmospheric organic and elemental carbon: The EUSAAR protocol. *Atmos. Meas. Tech.* **2010**, *3*, 79–89. [[CrossRef](#)]
32. Arhami, M.; Kuhn, T.; Fine, P.M.; Delfino, R.J.; Sioutas, C. Effects of Sampling Artifacts and Operating Parameters on the Performance of a Semicontinuous Particulate Elemental Carbon/ Organic Carbon Monitor. *Environ. Sci. Technol.* **2006**, *40*, 945–954. [[CrossRef](#)]